University of Baghdad
College of Engineering
JOURNAL OF ENGINEERING

Journal of Engineering
journal homepage: www.joe.uobaghdad.edu.iq
Number 1 Volume 28 January 2022

Mechanical and Energy Engineering

A Five Variable Refined Plate Theory For Thermal Buckling Analysis Uniform And Nonuniform Of Cross-Ply Laminated Plates

Hussein Atee Hashim
MSc student
Mechanical Engineering Department
College of Engineering
University of Baghdad
Iraq-Baghdad
H.alzadi1803M@coeng.uobaghdad.edu.iq

Ibtehal Abbas Sadiq
Asst. Professor
Mechanical Engineering Department
College of Engineering
University of Baghdad
Iraq-Baghdad
ibtehal.abbas@coeng.uobaghdad.edu.iq

ABSTRACT

This research is devoted to investigating the thermal buckling analysis behaviour of laminated composite plates subjected to uniform and non-uniform temperature fields by applying an analytical model based on a refined plate theory (RPT) with five unknown independent variables. The theory accounts for the parabolic distribution of the transverse shear strains through the plate thickness and satisfies the zero-traction boundary condition on the surface without using shear correction factors; hence a shear correction factor is not required. The governing differential equations and associated boundary conditions are derived by using the virtual work principle and solved via Navier-type analytical procedure to obtain critical buckling temperature. Results are presented for: uniform and linear cross-ply lamination with symmetry and antisymmetric stacking, simply supported boundary condition, different aspect ratio (a/b), various orthogonality ratio (E_1/E_2), varying ratios of coefficient of uniform and linear thermal expansion (α_2/α_1), uniform and linearly varying temperature thickness ratio (a/h) and numbers of layers on thermal buckling of the laminated plate. It can be concluded that this theory gives good results compared to other theories.

Keywords: Uniform and non-uniform thermal buckling, critical buckling temperature, five-variable refined plate theory

الانبعاج الحراري المنتظم وغير المنتظم للالواح ذات الطبقات المتقاطعة بأستخدام النظرية المحسنة ذات خمس متغييرات

حسين عاتي هاشم
طالب ماجستير
جامعة بغداد- كلية الهندسة- قسم هندسة الميكانيك

ابتهال عباس صادق
استاذ مساعد
جامعة بغداد – كلية الهندسة – قسم هندسة الميكانيك

الخلاصة

هذا البحث مخصص لدراسة سلوك تحليل الالتواء الحراري للألواح المركبة المصفحة ، المعرضة درجة حرارة منتظمة وغير منتظمة, من خلال تطبيق نموذج تحليلي يعتمد على نظرية الصفيحة المحسنة (RPT) مع خمسة متغيرات مستقلة غير معروفة. تفسر النظرية التوزيع

*Corresponding author
Peer review under the responsibility of University of Baghdad.
https://doi.org/10.31026/j.eng.2022.01.07

Article received: 29/6/2021
Article accepted: 22/8/2021
Article published:1/1/2022

المكافئ لسلالات القص المستعرضة من خلال سماكة اللوحة ، وتفي بشرط حدود الجر الصفري على السطح دون استخدام عوامل تصحيح القص ، وبالتالي فإن عامل تصحيح القص غير مطلوب. يتم اشتقاق المعادلات التفاضلية الحاكمة وشروط الحدود المرتبطة بها من خلال استخدام مبدأ العمل الافتراضي وحلها عبر إجراء تحليلي من نوع Navier للحصول على درجة حرارة الالتواء الحرجة لحالة الحدود المدعومة ببساطة للصفائح المتقاطعة المتناظرة وغير المتماثلة. يستخدم برنامج MATLAB 2018 لدراسة تأثير نسبة السماكة (a/h) ونسبة العرض إلى الارتفاع (a/b) ونسبة التعامد (E_1/E_2) ومعامل نسبة التمدد الحراري (α_2/α_1) وعدد الطبقات على الأنبعاج الحراري للصفائح الطبقية. يمكن الاستنتاج أن هذه النظرية تعطي نتائج جيدة عند مقارنتها بالنظريات الأخرى.

الكلمات الرئيسية: انبعاج حراري منتظم وغير منتظم, درجة حرارة الانبعاج الحرج, نظرية الصفائح المكررة ذات خمسة متغيرات

1. INTRODUCTION

Fiber-reinforced composite laminates, which have high strength-to-weight and stiffness-to-weight ratios, are becoming important in weight-sensitive applications such as aircraft and space vehicles. As a result, thermal buckling analysis of composite laminates is very important, especially in thin-walled members, since structural components of these highspeed machines are usually subjected to nonuniform temperature distribution due to aerodynamic and solar radiation heating**. (Chen, W. J., et al., 1991),** studied thermal buckling behaviour of composite laminated plates subjected to uniform or non-uniform temperature fields is analyzed with the aid of finite elements. **(Shi, et al., 1999),** developed the thermal post-buckling fabricated from thin composite plates using the method of finite element formulation in brand coordinates. The shapes of linear buckling modes used to model the post-buckling deflection studied post-buckling of laminations that are symmetrically laminated, antisymmetric angle ply, and investigated the stiffness and deflection unsymmetrically laminated composite plates subjected to mechanical and thermal loads. **(Mansour, M., et al., 2010),** Studied thermal buckling behavior of the symmetric cross-ply laminated rectangular thin plates subjected to uniform and or non-uniform temperature fields. based on differential quadrature method (DQM) is implemented for analysis. The procedure is divided into two stages: (1) solving the in-plane thermoelasticity problem to obtain the in-plane force resultants, and (2) solving the buckling problem using the force distribution obtained in the previous step. By discretizing, numerical solutions can be obtained. **(Le-Chung Shiau, et al., 2010)** studied the thermal buckling behavior of composite laminated plates by using the finite element method. The thermal buckling mode shapes of cross-ply and angle-ply laminates with various E_1/E_2 ratios, aspect ratios, fiber angle, stacking sequence and boundary condition were studied in detail. The results indicate that the high E_1/E_2 and a_2/a_1 ratios of AS4/3501-6 and T 300/5208 laminates produce higher bending rigidity along the fiber direction and higher in-plane compressive force in a direction perpendicular to the fiber direction. **(Nsaif and Jameel, 2013)** studied buckling analysis of composite laminates for critical thermal (uniform and linear) and thermo-mechanical loads. The analytical investigation involved certain mathematical preliminaries, a study of equations of orthotropic elasticity for classical laminated plate theory (CLPT), higher-order shear deformation plate theory (HSDT), and numerical analysis (Finite element method). The equation of motion is derived and solved using the Navier method and Levy method for symmetric and anti-symmetric cross-ply and angle-ply laminated plates to obtain buckling load by solving the eigenvalue problem for different boundary conditions under different

thermomechanical loading. The experimental investigation is to find mechanical properties at room temperature of glass-polyester. **(Bourada, M., et al., 2012)** performed an analysis of thermal buckling analysis on sandwich plates made of functionally graded material (FGM) using a novel four-variable refined plate theory. Thermal loads are assumed to be uniform, linear, and nonlinear, in addition to an overall rise in the thickness direction. **(Fazzolari, et al., 2013)** studied buckling of composite plate assemblies using higher-order shear deformation theory, an exact method of solution For the first time, a comprehensive use of symbolic algebra is developed to perform a buckling analysis on composite plate assemblies. To derive the governing differential equations and natural boundary conditions, the principle of minimum potential energy is applied. **(Fazzolari and Carrera, 2014)** investigated the thermal stability of functionally graded material (FGM) isotropic and sandwich plates using refined quasi-3D Equivalent Single Layer (ESL) and Zig-Zag (ZZ) plate models developed within the Carrera Unified Formulation (CUF) and implemented within the Hierarchical Trigonometric Ritz Formulation (HTRF).Uniform, linear, and non-linear temperature rises through-the-thickness direction are taken into account. **(Cetkovic, 2016)** studied thermal buckling of laminated composite plates based on layer-wise theory of reddy and a new version of layer-wise theory of Reddy. From the strong form, analytical solution is derived based on Navier's type, while the weak form is analysed using the isoperimetric finite element approximation. **(Xing and Wang, 2017)** investigated the critical buckling temperature of thin rectangular plates with functionally graded surfaces. Closed form solutions are obtained for the plate with a critical thermal parameter. different barrier conditions using the separation-of-variables method, under uniform, linear, and nonlinear temperature fields. **(Vescovini, R., et al., 2017)** discussed the analysis of composite plates and sandwich panels for thermal buckling using a Ritz-based variable-kinematic formulation applying refined, higher-order theories to specific regions, such as the core of sandwich panels, is possible. **(Sadiq and Majeed, 2019)** studied A new higher-order displacement field that is used to calculate the critical buckling temperature of an angle-ply laminated plate. The equations of motion for simply supported laminated plates based on higher-order theory angle-ply plates are derived using Hamilton's principle and solved using a Navier-type solution. **(Aditya Narayan, D., et al., 2019)** investigated thermoelastic buckling properties of variable stiffness composite shells, cylindrical and spherical shell frames subjected to uniform and non-uniform thermal fields are investigated using a finite element approach that incorporates higher-order theory accounting for the thickness effect. The critical buckling temperature is determined by solving the governing equations developed using the principle of energy minimization via the eigenvalue approach. **(Emmanuel Nicholas, P., et al., 2019)** optimized laminated composite plates subjected to nonuniform thermal loads, using the finite element method to analyze the plate during the optimization process. **(Balakrishna A., and Singh, B. N., 2020)** studied the thermal response of a laminated functionally graded carbon nanotube-reinforced composite (FG-CNTRC) plate structure under various types of non-uniform edge compression loading is predicted using finite element discretization and type polynomial-based higher-order shear deformation theory (HSDT). The application of non-uniform edge loads results in a non-uniform in-plane stress distribution. These in-plane stresses are determined using either

the finite element method or the in-plane elasticity approach. In present work, critical temperature of simply supported composite cross-ply plate is obtained using refined five-parameter plate theory (RPT). The significant advantage of our proposed theory is that five unknown variable exists in its displacement formula and governing equation. The effect of thickness ratio (a/h), aspect ratio(a/b), orthogonality ratio (E_1/E_2), coefficient of thermal expansion ratio (α_1/α_2) and numbers of layers on thermal buckling of laminated plate for symmetric and antisymmetric thin and thick plate are investigated.

2 .THEORETICAL ANALYSIS

2.1. Displacement field

Consider a rectangular plate of a total thickness (h) composed on (n) orthotropic layers with the coordinate system (see **Fig. 1**) **(S.-E. Kim, 2009)**. Refined plate theory fulfills equilibrium conditions at the plate's top and bottom forces without using a shear correction factor.

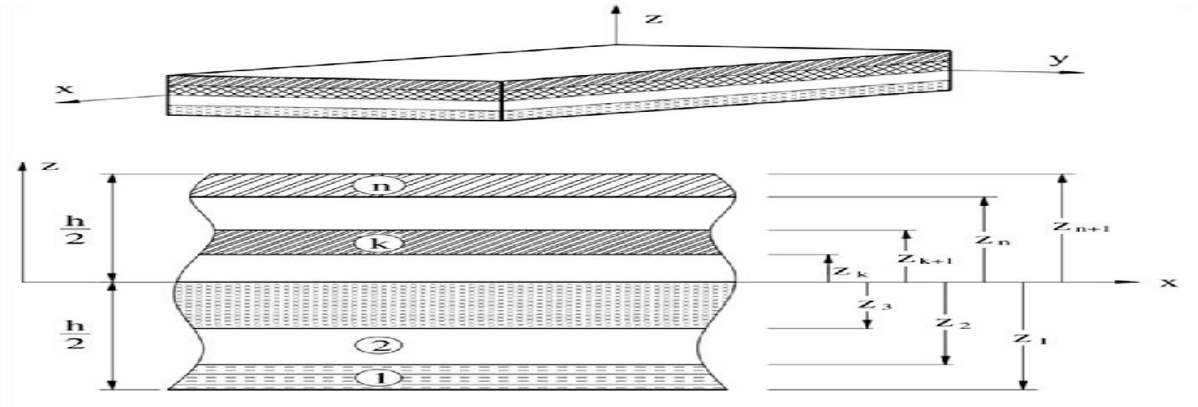

Figure 1. Coordinate system and layer numbering used for a typical laminated plate.

The oblique displacement W is composed of three components: extension wa, bending wb, and shear ws. According to **(Kim, S.-E., 2009)**, the displacement field can be expressed as follows:

$$U(x,y,z) = u(x,y) - z\left[\frac{\partial w_b}{\partial x}\right] + z\left[\frac{1}{4} - \frac{5}{3}\left(\frac{z}{h}\right)^2\right]\frac{\partial w_s}{\partial x}$$

$$V(x,y,z) = v(x,y) - z\left[\frac{\partial w_b}{\partial y}\right] + z\left[\frac{1}{4} - \frac{5}{3}\left(\frac{z}{h}\right)^2\right]\frac{\partial w_s}{\partial y}$$

$$W(x,y,z) = w_a(x,y) + w_b(x,y) + w_s(x,y) \quad (1)$$

For small strain Linear, the strain-displacement relations take the for **(Reddy, J. N., 2004)**

$$\mathcal{E}_x = \frac{\partial u}{\partial x}, \mathcal{E}_y = \frac{\partial v}{\partial y}, \mathcal{E}_{xy} = \frac{1}{2}\left(\frac{\partial u}{\partial y} + \frac{\partial v}{\partial x}\right) = \frac{1}{2}\gamma_{xy}, \mathcal{E}_{yz} = \frac{1}{2}\left(\frac{\partial v}{\partial z} + \frac{\partial w}{\partial y}\right) = \frac{1}{2}\gamma_{yz}, \mathcal{E}_{xz} = \frac{1}{2}\left(\frac{\partial u}{\partial z} + \frac{\partial w}{\partial x}\right) = \frac{1}{2}\gamma_{xz} \quad (2)$$

The strain components will be derived, based on the displacement Refined of plate, from eq. (1) and eq. (2) as:

$$\mathcal{E}_x = \frac{\partial u}{\partial x} - z\frac{\partial^2 w_b}{\partial x^2} + z\left[\frac{1}{4} - \frac{5}{3}\left(\frac{z}{h}\right)^2\right]\frac{\partial^2 w_s}{\partial x^2}, \mathcal{E}_y = \frac{\partial v}{\partial y} - z\frac{\partial^2 w_b}{\partial y^2} + z\left[\frac{1}{4} - \frac{5}{3}\left(\frac{z}{h}\right)^2\right]\frac{\partial^2 w_s}{\partial y^2}$$

$$\gamma_{xy} = \frac{\partial u}{\partial y} + \frac{\partial v}{\partial x} - 2z\left(\frac{\partial^2 w_b}{\partial x\,\partial y}\right) + 2z\left[\frac{1}{4} - \frac{5}{3}\left(\frac{z}{h}\right)^2\right]\frac{\partial^2 w_s}{\partial x\,\partial y}, \gamma_{yz} = \frac{\partial w_a}{\partial y} + \left[\frac{5}{4} - 5\left(\frac{z}{h}\right)^2\right]\frac{\partial w_s}{\partial y}$$

$$\gamma_{xz} = \frac{\partial w_a}{\partial x} + \left[\frac{5}{4} - 5\left(\frac{z}{h}\right)^2\right]\frac{\partial w_s}{\partial x} \quad (3)$$

The strains associated with the displacements are:

$$\mathcal{E}_x = \mathcal{E}_x^0 + zk_x^b + fk_x^s, \mathcal{E}_y = \mathcal{E}_y^0 + zk_y^b + fk_y^s, \gamma_{xy} = \gamma_{xy}^0 + zk_{xy}^b + fk_{xy}^s$$

$$\gamma_{yz} = \gamma_{yz}^a + g\gamma_{yz}^s, \gamma_{xz} = \gamma_{xz}^a + g\gamma_{xz}^s, \mathcal{E}_z = 0 \quad (4)$$

Where:

$$\begin{Bmatrix}\mathcal{E}_x^0\\ \mathcal{E}_y^0\\ \gamma_{xy}^0\end{Bmatrix} = \begin{Bmatrix}\frac{\partial u}{\partial x}\\ \frac{\partial v}{\partial y}\\ \frac{\partial u}{\partial y} + \frac{\partial v}{\partial x}\end{Bmatrix}, \begin{Bmatrix}k_x^b\\ k_y^b\\ k_{xy}^b\end{Bmatrix} = \begin{Bmatrix}-\frac{\partial^2 w_b}{\partial x^2}\\ -\frac{\partial^2 w_b}{\partial y^2}\\ -2\frac{\partial^2 w_b}{\partial x\,\partial y}\end{Bmatrix}, \begin{Bmatrix}k_x^s\\ k_y^s\\ k_{xy}^s\end{Bmatrix} = \begin{Bmatrix}-\frac{\partial^2 w_s}{\partial x^2}\\ -\frac{\partial^2 w_s}{\partial y^2}\\ -2\frac{\partial^2 w_s}{\partial x\,\partial y}\end{Bmatrix}, \begin{Bmatrix}\gamma_{xz}^a\\ \gamma_{yz}^a\end{Bmatrix} = \begin{Bmatrix}\frac{\partial w_a}{\partial x}\\ \frac{\partial w_a}{\partial y}\end{Bmatrix}, \begin{Bmatrix}\gamma_{xz}^s\\ \gamma_{yz}^s\end{Bmatrix} = \begin{Bmatrix}\frac{\partial w_s}{\partial x}\\ \frac{\partial w_s}{\partial y}\end{Bmatrix}$$

$$f = -\frac{1}{4}z + \frac{5}{3}z\left(\frac{z}{h}\right)^2, \quad g = \frac{5}{4} - 5\left(\frac{z}{h}\right)^2 \quad (5)$$

2.2 Hamilton's principle

Hamilton's principle is used herein to derive the equations of motion appropriate to the displacement field. The principle can be stated in analytical form as **(Reddy, J. N., 2004).**

$$0 = \int_0^T (\delta U + \delta V)dt \quad (6)$$

The strain energy δU can be written as:

$$\delta U = \int_V \left(\sigma_x \delta\mathcal{E}_x + \sigma_y \delta\mathcal{E}_y + \sigma_{xy}\delta\gamma_{xy} + \sigma_{yz}\delta\gamma_{yz} + \sigma_{xz}\delta\gamma_{xz}\right)dV \quad (7)$$

Substituting Eq. (4) into Eq. (7) we get:

$$\delta U = \int_V \left[\sigma_{xx}\left(\delta\mathcal{E}_x^0 + z\delta k_x^b + f\delta k_x^s\right) + \sigma_{yy}\left(\delta\mathcal{E}_y^0 + z\delta k_y^b + f\delta k_y^s\right) + \sigma_{xy}\left(\delta\gamma_{xy}^0 + z\delta k_{xy}^b + f\delta k_{xy}^s\right) + \sigma_{yz}\left(\delta\gamma_{yz}^a + g\delta\gamma_{yz}^s\right) + \sigma_{xz}\left(\delta\gamma_{xz}^a + g\delta\gamma_{xz}^s\right)\right]dV$$

$$\delta U = \int_A \left[N_x\delta\mathcal{E}_x^0 + N_y\delta\mathcal{E}_y^0 + N_{xy}\delta\gamma_{xy}^0 + M_x^b\delta k_x^b + M_y^b\delta k_y^b + M_{xy}^b\delta k_{xy}^b + M_x^s\delta k_x^s + M_y^s\delta k_y^s + M_{xy}^s\delta k_{xy}^s + Q_{yz}^a\delta\gamma_{yz}^a + Q_{xz}^a\delta\gamma_{xz}^a + Q_{yz}^s\delta\gamma_{yz}^s + Q_{xz}^s\delta\gamma_{xz}^s\right]\partial x\,\partial y \quad (8)$$

Substituting Eq. (5) in Eq. (8) and by using by parts integrating we get the final strain energy as below:

$$\delta U = -\int_A \left[\frac{\partial N_x}{\partial x}\delta u + \frac{\partial N_y}{\partial y}\delta v + \frac{\partial N_{xy}}{\partial y}\delta u + \frac{\partial N_{xy}}{\partial x}\delta v + \frac{\partial^2 M_x^b}{\partial x^2}\delta w_b + \frac{\partial^2 M_y^b}{\partial y^2}\delta w_b + 2\frac{\partial^2 M_{xy}^b}{\partial x\,\partial y}\delta w_b + \frac{\partial^2 M_x^s}{\partial x^2}\delta w_s + \frac{\partial^2 M_y^s}{\partial y^2}\delta w_s + 2\frac{\partial^2 M_{xy}^s}{\partial x\,\partial y}\delta w_s + \frac{\partial Q_{yz}^a}{\partial y}\delta w_a + \frac{\partial Q_{xz}^a}{\partial x}\delta w_a + \frac{\partial Q_{yz}^s}{\partial y}\delta w_s + \frac{\partial Q_{xz}^s}{\partial x}\delta w_s\right] \partial x\,\partial y \quad (9)$$

The Work done by applied thermal Forces can be written as:

$$\delta V = \int_A \left[N_x^T \frac{\partial^2 (w_a + w_b + w_s)}{\partial x^2} + N_y^T \frac{\partial^2 (w_a + w_b + w_s)}{\partial y^2} + 2N_{xy}^T \frac{\partial^2 (w_a + w_b + w_s)}{\partial x\,\partial y}\right] dA \quad (10)$$

2.3. Equation of motion

Substituting Eqs. (9)-(10) into Eq. (6) and then collecting the coefficient of $(\delta u, \delta v, \delta w_a, \delta w_b, \text{and } \delta w_s)$ to zero separately, the equation of motion for the ply plate are obtained as follows:

$$\delta u:\ \frac{\partial N_x}{\partial x} + \frac{\partial N_{xy}}{\partial y} = 0\,,\ \delta v:\ \frac{\partial N_y}{\partial y} + \frac{\partial N_{xy}}{\partial x} = 0\,,\ \delta w_b:\ \frac{\partial^2 M_x^b}{\partial x^2} + \frac{\partial^2 M_y^b}{\partial y^2} + 2\frac{\partial^2 M_{xy}^b}{\partial x\,\partial y} + N^T(\omega) = 0 \quad (11)$$

$$\delta w_s:\ \frac{\partial^2 M_x^s}{\partial x^2} + \frac{\partial^2 M_y^s}{\partial y^2} + 2\frac{\partial^2 M_{xy}^s}{\partial x\,\partial y} + \frac{\partial Q_{xz}^s}{\partial x} + \frac{\partial Q_{yz}^s}{\partial y} + N^T(\omega) = 0,\ \delta w_a:\ \frac{\partial Q_{xz}^a}{\partial x} + \frac{\partial Q_{yz}^a}{\partial y} + N^T(\omega) = 0 \quad (12)$$

The transformed stress-strain relations of an orthotropic lamina in a plane state of stress are **(Reddy J. N., 2004)**

$$\begin{Bmatrix}\sigma_x\\ \sigma_y\\ \sigma_{xy}\end{Bmatrix} = \begin{bmatrix}\bar{Q}_{11} & \bar{Q}_{12} & \bar{Q}_{16}\\ \bar{Q}_{12} & \bar{Q}_{22} & \bar{Q}_{26}\\ \bar{Q}_{16} & \bar{Q}_{26} & \bar{Q}_{66}\end{bmatrix}\left(\begin{Bmatrix}\varepsilon_x\\ \varepsilon_y\\ \gamma_{xy}\end{Bmatrix} - \begin{Bmatrix}\alpha_{xx}\\ \alpha_{yy}\\ 2\alpha_{xy}\end{Bmatrix}\Delta T\right), \begin{Bmatrix}\sigma_{yz}\\ \sigma_{xz}\end{Bmatrix} = \begin{bmatrix}\bar{Q}_{44} & \bar{Q}_{45}\\ \bar{Q}_{45} & \bar{Q}_{55}\end{bmatrix}\begin{Bmatrix}\gamma_{yz}\\ \gamma_{xz}\end{Bmatrix} \quad (13)$$

The force results are:

$$\begin{Bmatrix}\begin{Bmatrix}N_x\\ N_y\\ N_{xy}\end{Bmatrix}\\ \begin{Bmatrix}M_x^b\\ M_y^b\\ M_{xy}^b\end{Bmatrix}\\ \begin{Bmatrix}M_x^s\\ M_y^s\\ M_{xy}^s\end{Bmatrix}\end{Bmatrix} = \begin{bmatrix}A_{11} & A_{12} & A_{16} & B_{11} & B_{12} & B_{16} & B_{11}^s & B_{12}^s & B_{16}^s\\ A_{12} & A_{22} & A_{26} & B_{12} & B_{22} & B_{26} & B_{12}^s & B_{22}^s & B_{26}^s\\ A_{16} & A_{26} & A_{66} & B_{16} & B_{26} & B_{66} & B_{16}^s & B_{26}^s & B_{66}^s\\ B_{11} & B_{12} & B_{16} & D_{11} & D_{12} & D_{16} & D_{11}^s & D_{12}^s & D_{16}^s\\ B_{12} & B_{22} & B_{26} & D_{12} & D_{22} & D_{26} & D_{12}^s & D_{22}^s & D_{26}^s\\ B_{16} & B_{26} & B_{66} & D_{16} & D_{26} & D_{66} & D_{16}^s & D_{26}^s & D_{66}^s\\ B_{11}^s & B_{12}^s & B_{16}^s & D_{11}^s & D_{12}^s & D_{16}^s & H_{11}^s & H_{12}^s & H_{16}^s\\ B_{12}^s & B_{22}^s & B_{26}^s & D_{12}^s & D_{22}^s & D_{26}^s & H_{12}^s & H_{22}^s & H_{26}^s\\ B_{16}^s & B_{26}^s & B_{66}^s & D_{16}^s & D_{26}^s & D_{66}^s & H_{16}^s & H_{26}^s & H_{66}^s\end{bmatrix}\begin{Bmatrix}\begin{Bmatrix}\varepsilon_x^0\\ \varepsilon_y^0\\ \gamma_{xy}^0\end{Bmatrix}\\ \begin{Bmatrix}k_x^b\\ k_y^b\\ k_{xy}^b\end{Bmatrix}\\ \begin{Bmatrix}k_x^s\\ k_x^s\\ k_{xy}^s\end{Bmatrix}\end{Bmatrix}$$

$$\begin{Bmatrix} Q^a_{yz} \\ Q^a_{xz} \\ Q^s_{yz} \\ Q^s_{xz} \end{Bmatrix} = \begin{bmatrix} \mathrm{A}_{11} & \mathrm{A}_{11} & \mathrm{A}^{\mathrm{a}}_{44} & \mathrm{A}^{\mathrm{a}}_{45} \\ \mathrm{A}_{11} & \mathrm{A}_{11} & \mathrm{A}^{\mathrm{a}}_{45} & \mathrm{A}^{\mathrm{a}}_{55} \\ \mathrm{A}^{\mathrm{a}}_{44} & \mathrm{A}^{\mathrm{a}}_{45} & \mathrm{A}^{\mathrm{s}}_{44} & \mathrm{A}^{\mathrm{s}}_{45} \\ \mathrm{A}^{\mathrm{a}}_{45} & \mathrm{A}^{\mathrm{a}}_{55} & \mathrm{A}^{\mathrm{s}}_{45} & \mathrm{A}^{\mathrm{s}}_{55} \end{bmatrix} \begin{Bmatrix} \gamma^{\mathrm{a}}_{\mathrm{yz}} \\ \gamma^{\mathrm{a}}_{\mathrm{xz}} \\ \gamma^{\mathrm{s}}_{\mathrm{yz}} \\ \gamma^{\mathrm{s}}_{\mathrm{xz}} \end{Bmatrix}, \begin{Bmatrix} N^T_x \\ N^T_y \\ N^T_{xy} \end{Bmatrix} = \sum_{k=1}^{N} \int_{z_k}^{z_{k+1}} \begin{bmatrix} \bar{Q}_{11} & \bar{Q}_{12} & \bar{Q}_{16} \\ \bar{Q}_{12} & \bar{Q}_{22} & \bar{Q}_{26} \\ \bar{Q}_{16} & \bar{Q}_{26} & \bar{Q}_{66} \end{bmatrix} \begin{Bmatrix} \alpha_{xx} \\ \alpha_{yy} \\ 2\alpha_{xy} \end{Bmatrix} \Delta T \, dz$$

$$\begin{Bmatrix} M^T_x \\ M^T_y \\ M^T_{xy} \end{Bmatrix} = \sum_{k=1}^{N} \int_{z_k}^{z_{k+1}} \begin{bmatrix} \bar{Q}_{11} & \bar{Q}_{12} & \bar{Q}_{16} \\ \bar{Q}_{12} & \bar{Q}_{22} & \bar{Q}_{26} \\ \bar{Q}_{16} & \bar{Q}_{26} & \bar{Q}_{66} \end{bmatrix} \begin{Bmatrix} \alpha_{xx} \\ \alpha_{yy} \\ 2\alpha_{xy} \end{Bmatrix} \Delta T \, z \, dz$$

$\Delta T = \frac{\Delta T}{h}\left(z + \frac{h}{z}\right)$ for linear temperature rise, $\Delta T = T_f - T_i$ for the uniform temperature rise (14)

Eq. (12) can be expressed in terms of displacements (u, v, w_b, w_s, w_a) by substituting for the stress resultants from Eq. (14). the equations of motion (12) take the form:

$$\mathrm{A}_{11}\frac{\partial^2 \mathrm{u}}{\partial \mathrm{x}^2} + 2\mathrm{A}_{16}\frac{\partial^2 \mathrm{u}}{\partial \mathrm{x}\,\partial \mathrm{y}} + \mathrm{A}_{66}\frac{\partial^2 \mathrm{u}}{\partial \mathrm{y}^2} + \mathrm{A}_{16}\frac{\partial^2 \mathrm{v}}{\partial \mathrm{x}^2} + (\mathrm{A}_{16} + \mathrm{A}_{66})\frac{\partial^2 \mathrm{v}}{\partial \mathrm{x}\,\partial \mathrm{y}} + \mathrm{A}_{26}\frac{\partial^2 \mathrm{v}}{\partial \mathrm{y}^2} - \left[\mathrm{B}_{11}\frac{\partial^3 \mathrm{w_b}}{\partial \mathrm{x}^3} + 3\mathrm{B}_{16}\frac{\partial^3 \mathrm{w_b}}{\partial \mathrm{x}^2\,\partial \mathrm{y}} + (\mathrm{B}_{12} + 2\mathrm{B}_{66})\frac{\partial^3 \mathrm{w_b}}{\partial \mathrm{x}\,\partial \mathrm{y}^2} + \mathrm{B}_{26}\frac{\partial^3 \mathrm{w_b}}{\partial \mathrm{y}^3}\right] - \left[\mathrm{B}^{\mathrm{s}}_{11}\frac{\partial^3 \mathrm{w_s}}{\partial \mathrm{x}^3} + 3\mathrm{B}^{\mathrm{s}}_{16}\frac{\partial^3 \mathrm{w_s}}{\partial \mathrm{x}^2\,\partial \mathrm{y}} + (\mathrm{B}^{\mathrm{s}}_{12} + 2\mathrm{B}^{\mathrm{s}}_{66})\frac{\partial^3 \mathrm{w_s}}{\partial \mathrm{x}\,\partial \mathrm{y}^2} + \mathrm{B}^{\mathrm{s}}_{26}\frac{\partial^3 \mathrm{w_s}}{\partial \mathrm{y}^3}\right] = 0$$

$$\mathrm{A}_{16}\frac{\partial^2 \mathrm{u}}{\partial \mathrm{x}^2} + (\mathrm{A}_{12} + \mathrm{A}_{66})\frac{\partial^2 \mathrm{u}}{\partial \mathrm{x}\,\partial \mathrm{y}} + \mathrm{A}_{26}\frac{\partial^2 \mathrm{u}}{\partial \mathrm{y}^2} + \mathrm{A}_{66}\frac{\partial^2 \mathrm{v}}{\partial \mathrm{x}^2} + 2\mathrm{A}_{26}\frac{\partial^2 \mathrm{v}}{\partial \mathrm{x}\,\partial \mathrm{y}} + \mathrm{A}_{22}\frac{\partial^2 \mathrm{v}}{\partial \mathrm{y}^2} - \left[\mathrm{B}_{16}\frac{\partial^3 \mathrm{w_b}}{\partial \mathrm{x}^3} + (\mathrm{B}_{12} + 2\mathrm{B}_{66})\frac{\partial^3 \mathrm{w_b}}{\partial \mathrm{x}^2\,\partial \mathrm{y}} + 3\mathrm{B}_{26}\frac{\partial^3 \mathrm{w_b}}{\partial \mathrm{x}\,\partial \mathrm{y}^2} + \mathrm{B}_{22}\frac{\partial^3 \mathrm{w_b}}{\partial \mathrm{y}^3}\right] - \left[\mathrm{B}^{\mathrm{s}}_{16}\frac{\partial^3 \mathrm{w_s}}{\partial \mathrm{x}^3} + (\mathrm{B}^{\mathrm{s}}_{12} + 2\mathrm{B}^{\mathrm{s}}_{66})\frac{\partial^3 \mathrm{w_s}}{\partial \mathrm{x}^2\,\partial \mathrm{y}} + 3\mathrm{B}^{\mathrm{s}}_{26}\frac{\partial^3 \mathrm{w_s}}{\partial \mathrm{x}\,\partial \mathrm{y}^2} + \mathrm{B}^{\mathrm{s}}_{22}\frac{\partial^3 \mathrm{w_s}}{\partial \mathrm{y}^3}\right] = 0$$

$$B_{11}\frac{\partial^3 u}{\partial x^3} + 3B_{16}\frac{\partial^3 u}{\partial x^2 \partial y} + (B_{12} + 2B_{66})\frac{\partial^3 u}{\partial x \partial y^2} + B_{26}\frac{\partial^3 u}{\partial y^3} + B_{16}\frac{\partial^3 v}{\partial x^3} + (B_{12} + 2B_{66})\frac{\partial^3 v}{\partial x^2 \partial y} + 3B_{26}\frac{\partial^3 v}{\partial x \partial y^2} + B_{22}\frac{\partial^3 v}{\partial y^3} - \left[D_{11}\frac{\partial^4 w_b}{\partial x^4} + 4D_{16}\frac{\partial^4 w_b}{\partial x^3 \partial y} + 2(D_{12} + 2D_{66})\frac{\partial^4 w_b}{\partial x^2 \partial y^2} + 4D_{26}\frac{\partial^4 w_b}{\partial x \partial y^3} + D_{22}\frac{\partial^4 w_b}{\partial y^4}\right] - \left[D^s_{11}\frac{\partial^4 w_s}{\partial x^4} + 4D^s_{16}\frac{\partial^4 w_s}{\partial x^3 \partial y} + 2(D^s_{12} + 2D^s_{66})\frac{\partial^4 w_s}{\partial x^2 \partial y^2} + 4D^s_{26}\frac{\partial^4 w_s}{\partial x \partial y^3} + D^s_{22}\frac{\partial^4 w_s}{\partial y^4}\right] + \mathrm{N}^T(\omega) = 0$$

$$\mathrm{B}^{\mathrm{s}}_{11}\frac{\partial^3 \mathrm{u}}{\partial \mathrm{x}^3} + 3\mathrm{B}^{\mathrm{s}}_{16}\frac{\partial^3 \mathrm{u}}{\partial \mathrm{x}^2\,\partial \mathrm{y}} + (\mathrm{B}^{\mathrm{s}}_{12} + 2\mathrm{B}^{\mathrm{s}}_{66})\frac{\partial^3 \mathrm{u}}{\partial \mathrm{x}\,\partial \mathrm{y}^2} + \mathrm{B}^{\mathrm{s}}_{26}\frac{\partial^3 \mathrm{u}}{\partial \mathrm{y}^3} + \mathrm{B}^{\mathrm{s}}_{16}\frac{\partial^3 \mathrm{v}}{\partial \mathrm{x}^3} + (\mathrm{B}^{\mathrm{s}}_{12} + 2\mathrm{B}^{\mathrm{s}}_{66})\frac{\partial^3 \mathrm{v}}{\partial \mathrm{x}^2\,\partial \mathrm{y}} + 3\mathrm{B}^{\mathrm{s}}_{26}\frac{\partial^3 \mathrm{v}}{\partial \mathrm{x}\,\partial \mathrm{y}^2} + \mathrm{B}^{\mathrm{s}}_{22}\frac{\partial^3 \mathrm{v}}{\partial \mathrm{y}^3} - \left[\mathrm{D}^{\mathrm{s}}_{11}\frac{\partial^4 \mathrm{w_b}}{\partial \mathrm{x}^4} + 4\mathrm{D}^{\mathrm{s}}_{16}\frac{\partial^4 \mathrm{w_b}}{\partial \mathrm{x}^3\,\partial \mathrm{y}} + 2(\mathrm{D}^{\mathrm{s}}_{12} + 2\mathrm{D}^{\mathrm{s}}_{66})\frac{\partial^4 \mathrm{w_b}}{\partial \mathrm{x}^2\,\partial \mathrm{y}^2} + 4\mathrm{D}^{\mathrm{s}}_{26}\frac{\partial^4 \mathrm{w_b}}{\partial \mathrm{x}\,\partial \mathrm{y}^3} + \mathrm{D}^{\mathrm{s}}_{22}\frac{\partial^4 \mathrm{w_b}}{\partial \mathrm{y}^4}\right] - \left[\mathrm{H}^{s}_{11}\frac{\partial^4 w_s}{\partial x^4} + 4\mathrm{H}^{s}_{16}\frac{\partial^4 w_s}{\partial x^3 \partial y} + 2(\mathrm{H}^{s}_{12} + 2\mathrm{H}^{s}_{66})\frac{\partial^4 w_s}{\partial x^2 \partial y^2} + 4\mathrm{H}^{s}_{26}\frac{\partial^4 w_s}{\partial x \partial y^3} + \mathrm{H}^{s}_{22}\frac{\partial^4 w_b}{\partial y^4}\right] + A^a_{55}\frac{\partial^2 w_a}{\partial x^2} + A^a_{44}\frac{\partial^2 w_a}{\partial y^2} + 2A^a_{45}\frac{\partial^2 w_a}{\partial x \partial y} + A^s_{55}\frac{\partial^2 w_s}{\partial x^2} + A^s_{44}\frac{\partial^2 w_s}{\partial y^2} + 2A^s_{45}\frac{\partial^2 w_s}{\partial x \partial y} + \mathrm{N}^T(\omega) = 0$$

$$\mathrm{A}_{55}\frac{\partial^2 \mathrm{w_a}}{\partial \mathrm{x}^2} + \mathrm{A}_{44}\frac{\partial^2 \mathrm{w_a}}{\partial \mathrm{y}^2} + 2\mathrm{A}_{45}\frac{\partial^2 \mathrm{w_a}}{\partial \mathrm{x}\,\partial \mathrm{y}} + \mathrm{A}^{\mathrm{a}}_{55}\frac{\partial^2 \mathrm{w_s}}{\partial \mathrm{x}^2} + \mathrm{A}^{\mathrm{a}}_{44}\frac{\partial^2 \mathrm{w_s}}{\partial \mathrm{y}^2} + 2\mathrm{A}^{\mathrm{a}}_{45}\frac{\partial^2 \mathrm{w_s}}{\partial \mathrm{x}\,\partial \mathrm{y}} + \mathrm{N}^T(\omega) = 0 \quad (15)$$

2.4. Navier solution

In Navier's method, the generalized displacements are expanded into a double trigonometric series in terms of unknown parameters. The choice of function in the series is restricted to those that satisfy the problem's boundary condition. The Navier method is employed to obtain the closed-

form solutions of the partial differential equations in Eq. (12) for simply supported rectangular plates. Two types of simply supported boundary conditions are **(Reddy J. N., 2004)**

2.4.1 Navier Solution of Cross-Ply Laminated Plates

Assuming the following displacements form to satisfied simply supported boundary conditions for cross-ply

$$u = \sum_{m=1}^{\infty}\sum_{n=1}^{\infty} U_{mn}\cos\alpha x \sin\beta y,\ v = \sum_{m=1}^{\infty}\sum_{n=1}^{\infty} V_{mn}\sin\alpha x\cos\beta y$$

$$W_b = \sum_{m=1}^{\infty}\sum_{n=1}^{\infty} W_{bmn}\sin\alpha x\sin\beta y,\ W_s = \sum_{m=1}^{\infty}\sum_{n=1}^{\infty} W_{smn}\sin\alpha x\sin\beta y$$

$$W_a = \sum_{m=1}^{\infty}\sum_{n=1}^{\infty} W_{amn}\sin\alpha x\sin\beta y \quad (16)$$

3. EIGENVALUE PROBLEM

Equations of motion Eq. (12) can be expressed in terms of displacements by substituting the force and moment resultants from Eq. (14) and using Eq. (15), from using boundary conditions for cross-ply result an eigenvalue as follows.

$$\begin{bmatrix} s_{11} & s_{12} & s_{13} & s_{14} & 0 \\ s_{12} & s_{22} & s_{23} & s_{24} & 0 \\ s_{13} & s_{23} & s_{33}-C & s_{34}-C & -C \\ s_{14} & s_{24} & s_{34}-C & s_{44}-C & s_{45}-C \\ 0 & 0 & -C & s_{45}-C & s_{55}-C \end{bmatrix} \begin{Bmatrix} U_{mn} \\ V_{mn} \\ W_{bmn} \\ W_{smn} \\ W_{amn} \end{Bmatrix} = 0 \quad (17)$$

And s_{ij} is the element of stiffness.

4. NUMERICAL RESULTS AND DISCUSSION

Thermal buckling analysis of cross-ply plates under uniform and non-uniform temperature distribution is obtained by program above analytical solution of the refined theory using MATLAB 18. as shown in **Fig. 2**

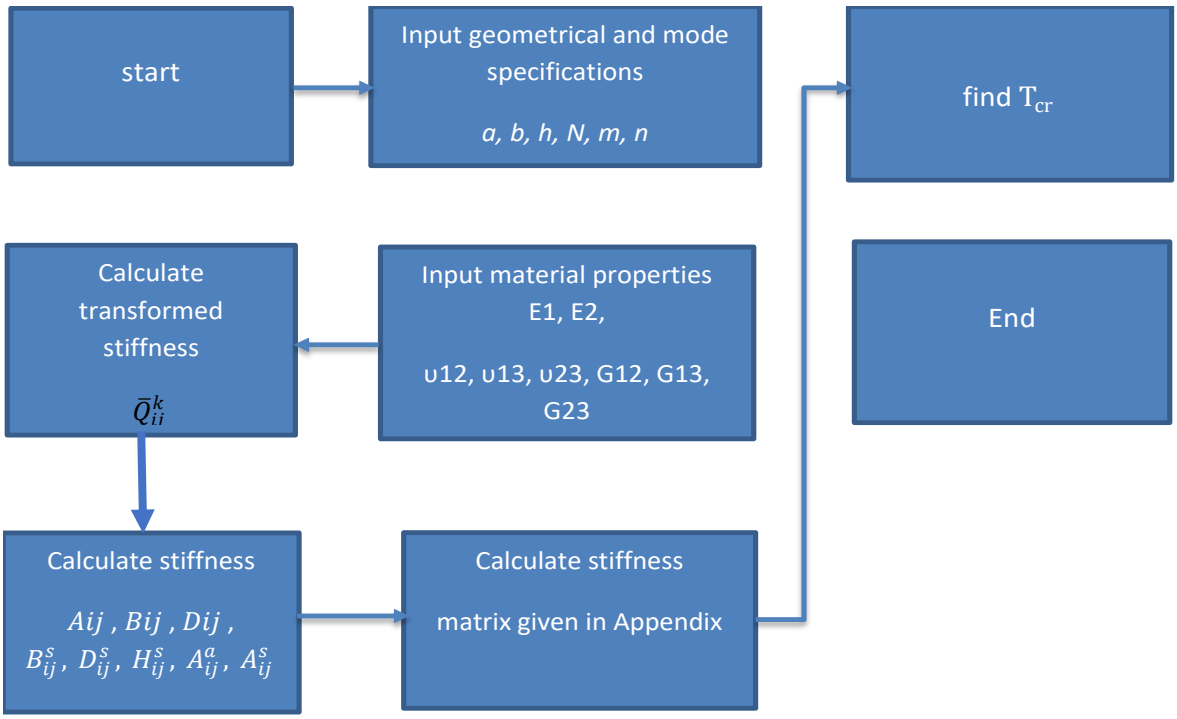

Figure 2. Flow chart for computer programming.

4.1 Cross-ply laminated plate under uniform temperature distribution.

4.1.1 Verification of results

In the present work, the results are verified by comparison with the numerical results obtained with different theories such as FSDT, HSDT, and refined four parameters plate theory. Thermal buckling for a uniform temperature rise of simply supported square plate cross-ply (0/90/90/0) laminated plate for material 1 was analyzed and listed in **Table 1.** material 1: $\frac{a}{h} = open$, $\frac{E_1}{E_2} = 25$, $E_2 = 1$, $\frac{G_{12}}{E_2} = 0.5$, $\frac{G_{13}}{E_2} = 0.5$, $\frac{G_{23}}{E_2} = 0.2, v_{12} = v_{13} = v_{23} = 0.25$, $\frac{\alpha_2}{\alpha_1} = 3, \alpha_1 = 1$

The critical temperature is normalized $T_{cr} = \left(\frac{a^2 h}{\pi^2 D_{22}} * T\right)$. Results show that while the present model of refined plate theory utilized more displacement parameters (five parameters), it is generally more accurate than (RPT) and less accurate than other higher-order theories.

Table 1. A critical temperature of cross-ply (0/90/90/0) simply supported square plate.

a/h	Present	LWT[1]	FSDT[2]	HSDT[3]	HSDT[4]	GRT[5]			
						RPT	RPT	RPT	RPT
4	0.06652	0.0514	0.0613	0.0570	0.0554	0.0711	0.05580	0.05888	0.06109

10	0.1658	0.1400	0.1598	0.1479	0.1436	0.1749	0.14784	0.15344	0.15704
20	0.2121	0.1976	/	0.2088	/	/	/	/	/
50	0.23029	0.2245	/	0.2383	/	/	/	/	/
100	0.2331	0.2291	0.2438	0.2432	0.2431	0.2440	0.24331	0.24378	0.24359

[1]Cetkovic, M., 2016; [2] Shukla, K. K., 2001; [3]Singh S., Singh J., and Shukla K. K., 2013; [4]Shu XP, Sun LX. (1994); [5]Mansouri MH, Shariyat M., 2014

Table 2 and **Table3** show the effects thickness ratio (a/h) on the critical temperature cross-ply of (0/90) and (0/90/0) simply supported square plate (a/b = 1) and subjected to uniform temperature respectively, observed that critical temperature decrease with increasing thickness ratio. Material properties for these tables as given as Material 2: $\frac{a}{h} = open$, $\frac{E_1}{E_2} = 15, E_2 = 1Gpa, \frac{G_{12}}{E_2} = 0.5, \frac{G_{23}}{E_2} = 0.3356, \nu_{12} = 0.3, \nu_{23} = 0.49, \frac{\alpha_1}{\alpha_0} = 0.015, \frac{\alpha_2}{\alpha_0} = 1, \alpha_0 = 10^{-6}$, The critical temperature is normalized in the following form ($T_{cr} = \alpha_0 T$).

Table 2. Normalized critical temperature of cross-ply (0/90) simply supported square plate (*a / b = 1*)

theory	a/h							
	2	10/3	4	5	20/3	10	20	100
Present	0.3544	0.2320	0.1880	0.1394	0.0895	0.0443	0.0119	4.8657e-4
LWT[1]	0.3695	0.2391	0.1926	0.1419	0.09052	0.04449	0.01188	0.4858e-3
HSDT[2]	0.3198	0.2114	0.1729	0.1302	0.08524	0.04310	0.01177	0.4856e-3

[1]Cetkovic, M., 2016; [2]Matsunaga, H., 2005

Table 3. A critical temperature of cross-ply (0/90/0) simply supported square plate (a /b =1)

Theory	a/h							
	2	10/3	4	5	20/3	10	20	100
Present	0.3351	0.2589	0.2261	0.1840	0.1318	0.0729	0.0214	9.0713e-4
LWT[1]	0.3595	0.2625	0.2272	0.1848	0.1340	0.07628	0.02316	0.9964e-3
NoorAK,3D[2]	/	/	0.2140	0.1763	/	0.07467	0.02308	0.9961e-3

[1]Cetkvic, M., 2016; [2]Noor A.K.,3D

Fig.3(a) and **Fig.3(b)** present the effect of aspect ratio (a/b) and thermal expansion ratio (α_2/α_1) cross-ply $(0/90)_s$ laminated plate on thermal buckling temperature. The results show good

agreement with other theories (M. Cetkovic 2016 and Kari RT, Palaninathan and Ramachandran J. 1989). **Material 3**: $\frac{E_1}{E_2} = 20, E_2 = 1, \frac{G_{12}}{E_2} = 0.5, \frac{G_{13}}{E_2} = 0.5, \frac{G_{23}}{E_2} = 0.5, v_{12} = v_{13} = v_{23} = 0.25, \frac{\alpha_2}{\alpha_1} = 2, \alpha_1 = 0.1 \times 10^{-5}$, a/h = 100.

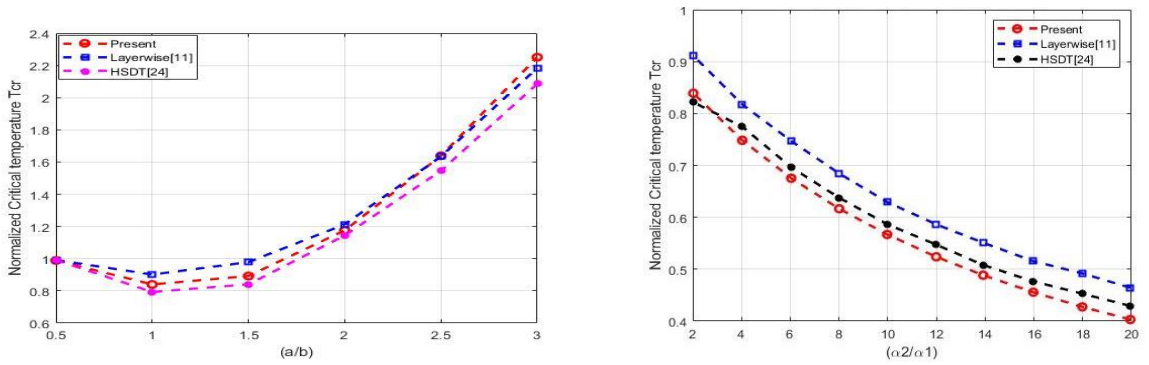

(a) Effect of aspect ratio (a/b) (b) thermal expansion coefficient (α_2/α_1) ratio

Figure 3. Effect of aspect ratio (a/b) and the ratio of thermal expansion coefficient (α_2/α_1) of cross-ply (0/90/90/0) Plate on thermal buckling temperature T_{cr}

4.1.2 Effect of design parameters

The effect of design parameters affecting the cross-critical ply's buckling temperature laminated thick and thin plate are analyzed such as symmetric and antisymmetric ply, number of layers, orthotropy ratio (E_1/E_2), thermal expansion coefficient ratio (α_2/α_1) under uniform temperature distribution.

Table 4 shows the effect of changing the thermal expansion coefficient ratio (α_2/α_1) on critical buckling temperature of four symmetric cross-ply (0/90/90/0) plates for different thickness ratio (a/h), the critical temperature decrease when (α_2/α_1) increase. The mechanical properties are the same in **Table 1.**

Changing of aspect ratio (a/b) effect on critical buckling temperature of four symmetric and antisymmetric cross-ply (0/90/90/0) laminated thick and thin plates are listed in **Table 5,** which shows that normalized critical temperature increases as aspect ratio (a/b) increase along with the thickness ratio. The mechanical properties are the same in **Table 1.**

Table 4. Effect (α_2/α_1) on critical temperature of cross-lamina (0/90)s simply supported square plate.

a/h	T_{cr}				
	(α_2/α_1)				
	2	4	6	8	10
5	0.09357	0.0851	0.07806	0.07208	0.06696

10	0.1741	0.1583	0.14519	0.13408	0.1245
15	0.2076	0.1888	0.1732	0.1599	0.14858
20	0.2227	0.2025	0.1858	0.1715	0.15937
50	0.2417	0.2199	0.2016	0.1862	0.17298
100	0.2447	0.2226	0.2041	0.18852	0.17512

Table 5. thermal buckling of symmetric and antisymmetric cross-lamina $[0/90]_N$ thick and thin plates for different aspect ratios simply supported.

Lay-up	a/h	T_{cr}			
		a/b			
		1	2	3	4
$[0/90]_s$	4	0.0665	0.07156	0.08053	0.08737
	10	0.1658	0.2019	0.2872	0.36024
	20	0.2122	0.2777	0.47497	0.70769
	100	0.2331	0.31608	0.6037	1.0376
$[0/90]_2$	4	0.0192	0.0252	0.0283	0.0301
	10	0.0455	0.09215	0.1268	0.1468
	20	0.0569	0.1542	0.2773	0.3799
	100	0.06189	0.19736	0.4558	0.8133

Table 6. shows the effect of changing (E_1/E_2) on critical temperature for four, eight, and twenty layers symmetric and antisymmetric cross-ply plates for different thickness ratio (a/h), notice that normalized critical temperature decrease when orthotropic ratio increases for both cross-ply symmetric and antisymmetric laminated plates (D_{22} increase). Using the mechanical properties are the same in **Table 1.**

Figs. 4(a)-(d) demonstrates four thermal buckling modes (a/h=10) rectangular (a/b=2) laminated plates that are simply supported.

Table 6. Effect (E_1/E_2) on thermal buckling of symmetric and antisymmetric cross lmina $[0/90]_N$ thick and thin

Lay-up		E_1/E_2	T_{cr} a/h			
			5	10	20	100
Symmetric	$[0/90]_s$	10	0.2341	0.3493	0.3988	0.4178
		20	0.1169	0.2048	0.2531	0.2737
		40	0.0469	0.0997	0.1400	0.1610
		50	0.0336	0.0761	0.1127	0.1333
	$[0/90]_{2s}$	10	0.1322	0.1973	0.2253	0.2360
		20	0.0574	0.1006	0.1243	0.1345
		40	0.0210	0.0447	0.0627	0.0721
		50	0.0147	0.0334	0.0494	0.0585
	$[0/90]_{5s}$	10	0.1048	0.1565	0.1787	0.1872
		20	0.0440	0.0771	0.0952	0.1031
		40	0.0158	0.0335	0.0471	0.0542
		50	0.0110	0.0250	0.0370	0.0438
Antisymmetric	$[0/90]_2$	10	0.0854	0.1246	0.1410	0.1471
		20	0.0349	0.0590	0.0715	0.0767
		40	0.0124	0.0253	0.0345	0.0390
		50	0.0087	0.0188	0.0269	0.0313
	$[0/90]_5$	10	0.0910	0.1354	0.1544	0.1617
		20	0.0375	0.0654	0.0806	0.0871
		40	0.0133	0.0282	0.0395	0.0453
		50	0.0093	0.02100	0.0309	0.0365

	$[0/90]_{10}$	10	0.0918	0.1370	0.1564	0.1638
		20	0.0379	0.0664	0.0819	0.0886
		40	0.0135	0.0286	0.0402	0.0462
		50	0.0094	0.02131	0.0315	0.0372

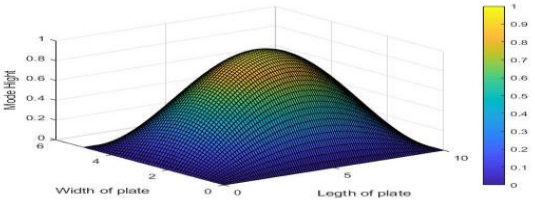

(a) (m =1, n = 1)

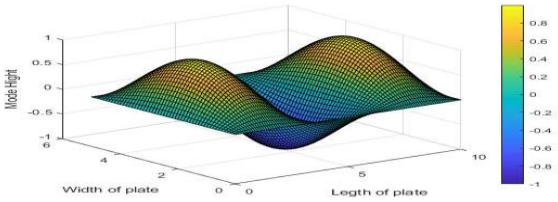

(c) (m =1, n = 3)

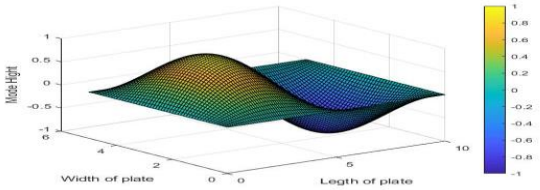

(b) (m =1, n = 2)

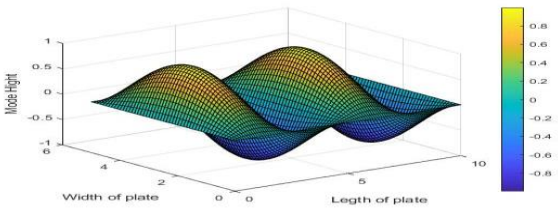

(d) (m =1, n = 4)

Figure 4 Thermal buckling mode for symmetric cross-ply (0/90/90/0) square plate, No. of layers = 4, a/h=10

4.2 Cross-ply laminated plate under nonuniform temperature distribution

4.2.1 Verification of results

The accuracy of the suggested solution of cross-ply plates under non-uniform temperature distribution is demonstrated using MATLAB 18 is program compared the results with other theories, which give good agreement as shown in **Table 7.** and **Table 8.** The critical temperature acquired when the temperature distribution is linearly varying is twice that obtained when the temperature distribution is uniform. This is because the thermal stress produced by a linearly varying temperature is half that of a constant temperature. **Fig. 5** shows the comparison between **(Cetkovic, M., 2016)** and the present work for the isotropic ceramic plate that is thin (a/h = 100) of simply supported boundary condition which displays the influence of changing aspect ratio (a/b) on critical buckling temperature.

Table 7. Critical temperature of an isotropic plate when it is subjected to various temperature distributions

Temperature rise	Present	LWT[1]	FSDT[2]	CLPT[3]	FSDT[4]	FSDT[5]	LW[6]
Uniform	57.5329	63.3	63.3	63.3	63.3	63.2	62.1
Lineary varying	132.76	126.5	/	126.0	/	/	/

[1]Cetkovic, M., 2016,[2]Bouazza, M., 1994, [3]Kari R.T.,[4]Maloy K.S. 2001, [5]Prabhu M. R., [6]Shariyat, M., 2007

Table 8. Critical temperature convergence of isotropic ceramic plates with varying a / h ratios

theory		a/h					
	10	10	20	40	60	80	100
uniform	CLPT[1]	1709.911	427.477	106.869	47.497	26.717	17.099
	FSDT[2]	1593.902	419.739	106.370	47.396	26.684	17.084
	HSDT[1]	1617.484	421.516	106.492	47.424	26.693	17.088
	LWT[3]	1633.155	422.513	106.556	47.436	26.698	17.091
	Present	1455.5	382.4013	96.8331	43.1400	24.2866	15.5494
Linear	CLPT[1]	3409.821	844.955	203.738	84.995	43.434	24.198
	FSDT[2]	/	/	/	/	/	/
	HSDT[1]	3224.968	833.032	202.984	84.848	43.387	24.177
	LWT[3]	3266.311	845.027	213.113	94.871	53.395	34.182
	Present	3358.94	882.464	223.460	99.553	56.045	35.883

[1]Javaheri R, Elsami MR., [2]Chen CS, Lin CY, Chien RD., [3]M. Cetkovic 2016,

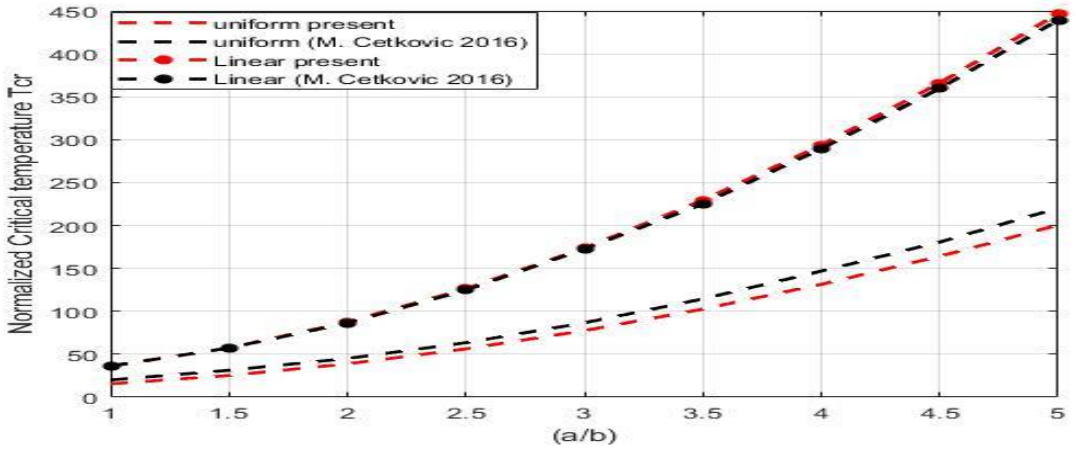

Figure 5. Effect of aspect ratio (a/b) of cross-ply (0/90/90/0) Plate for (a/h =100) on critical buckling

4.2.2 Effect of design parameters

The effect of many thick and thin plate parameters such as aspect ratio (a/b), (E_1/E_2) ratio, (α_2/α_1) ratio, number of layers for symmetric and antisymmetric cross-ply on critical buckling (T_{cr}) under linearly temperature distribution along the thickness are considered.

Note that the mechanical properties and nondimensional critical temperature for all tables and figures used in this section are material 1. The results listed of (a/h) and (E_1/E_2) are inverse because it is divided by D_{22}).

Table 9 and **Fig. 6** show the effect of thickness ratio on critical temperature under a different form of temperature distribution; as expected, the critical temperature obtained for the case of linearly varying temperature distribution is about double the critical temperature for the uniform temperature distribution.

Symmetric and antisymmetric cross-ply $(0/90)_2$, $(0/90)_3$ and $(0/90)_4$ for thick and thin plate on critical temperature listed in **Table 10**, which shows that normalized critical temperature increases as thickness ratio increase (D_{22}) increase, but it decreases when number of layer increase for symmetric cross-ply and its larger for antisymmetric laminated plate.

Table 9. Critical temperature ($T_{cr}a^2h/\pi^2D_{22}$) for cross-ply (0/90/90/0) simply supported square plate.

a/h	T_{cr}	
	uniform	Nonuniform
5	0.10919	0.2069
10	0.1816	0.3849
20	0.21830	0.4925
40	0.2299	0.5297
60	0.2322	0.5372
80	0.2330	0.5399
100	0.2334	0.5412

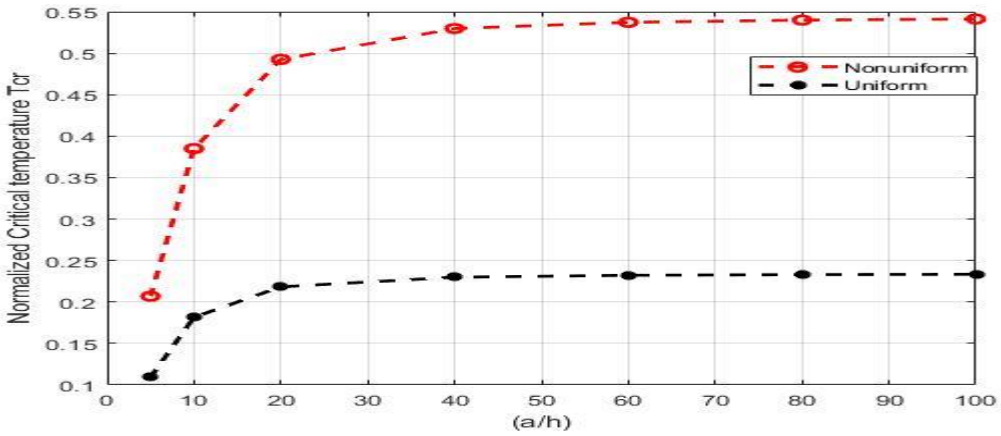

Figure 6. Critical temperature Tcr for a cross-ply $(0/90)_s$ simply supported plate

Table 10. nonuniform critical temperature for symmetric and antisymmetric cross-ply simply supported square plate.

a/h	T_{cr}					
	symmetric cross-ply			Antisymmetric cross-ply		
	$(0/90)_2$	$(0/90)_3$	$(0/90)_4$	$(0/90)_2$	$(0/90)_3$	$(0/90)_4$
5	0.2069	0.1132	0.0955	0.0560	0.0588	0.0598
10	0.3849	0.2105	0.1778	0.1003	0.1077	0.1103
20	0.4925	0.2694	0.2275	0.1255	0.1366	0.1404
40	0.5297	0.2898	0.2447	0.1339	0.1464	0.1508
60	0.5372	0.2939	0.2481	0.1356	0.1484	0.1529
80	0.5399	0.2954	0.2494	0.1362	0.1491	0.1536
100	0.5412	0.2961	0.2500	0.1365	0.1495	0.1539

Table 11 shows the effect of changing (E_1/E_2) on critical temperature symmetric cross-ply $(0/90)_s$ and $(0/90)_{2s}$ for thick and thin plates. Since stiffness increases when the orthotropic ratio increases, therefore, normalized critical temperature decrease (D_{22} increase).

Table 12. shows the effect of changing ($\alpha 2/\alpha 1$) on critical temperature symmetric cross-ply $(0/90)_s$ and $(0/90)_{2s}$thermal expansion coefficient ratio increase, therefore normalized critical temperature decreasing.

Changing aspect ratio (a/b) effect on critical buckling temperature of four and eight symmetric cross-ply (0/90/90/0) laminated thick and thin plates are listed in **Table 13**, which shows that critical temperature increases as aspect ratio (a/b) increases, also it increases with increasing (a/h) ratio which effected critical temperature larger than (a/b) ratio.

Table 11. Effects E_1/E_2 on the dimensionless buckling temperature of the square simply supported

No. of layer	a/h	T_{cr}				
		E_1/E_2				
		10	15	25	30	40
	5	0.5386	0.2710	0.2069	0.1632	0.1092
	10	0.8038	0.6044	0.3849	0.3196	0.2322

$(0/90)_s$	20	0.9177	0.7188	0.4925	0.4226	0.3260
	50	0.9558	0.7592	0.5345	0.4648	0.3679
	100	0.9614	0.7653	0.5412	0.4716	0.3748
$(0/90)_{2s}$	5	0.2987	0.1876	0.0955	0.0735	0.0475
	10	0.4459	0.3058	0.1778	0.1438	0.1010
	20	0.5091	0.3637	0.2275	0.1902	0.1418
	50	0.5302	0.3841	0.2469	0.2092	0.1600
	100	0.5333	0.3872	0.2500	0.2123	0.1630

Table 12. Effects (α_2/α_1) on the dimensionless buckling temperature of the square simply supported

No. of layer	α_2/α_1	T_{cr}				
		a/h				
		5	10	20	50	100
$(0/90)_s$	4	0.1970	0.3665	0.4691	0.5091	0.5154
	6	0.1799	0.3347	0.4283	0.4649	0.4706
	8	0.1655	0.3079	0.3940	0.4277	0.4330
	100	0.0353	0.0658	0.0842	0.0914	0.0925
$(0/90)_{2s}$	4	0.0912	0.1697	0.2171	0.2357	0.2386
	6	0.0836	0.1555	0.1990	0.2160	0.2186
	8	0.0771	0.1435	0.1836	0.1993	0.2018
	100	0.0169	0.0315	0.0404	0.0438	0.0443

Table 13. linear temperature of antisymmetric cross-lamina $(0/90)_N$ to different aspect ratio simply supported.

No. of layer	a/b	T_{cr}				
		a/h				
		5	10	20	50	100

$(0/90)_2$	1	0.0560	0.1003	0.1255	0.1350	0.1365
	2	0.0721	0.1836	0.3072	0.3799	0.3932
	3	0.0808	0.2447	0.5352	0.8137	0.8796
	4	0.0858	0.2797	0.7239	1.3540	1.5495
$(0/90)_4$	1	0.0598	0.1103	0.1404	0.1521	0.1539
	2	0.0775	0.2026	0.3495	0.4401	0.4571
	3	0.0865	0.2675	0.6041	0.9472	1.0316
	4	0.09149	0.3037	0.8082	1.5714	1.8206

5. CONCLUSIONS

Thermal buckling analysis of cross-ply laminated thick and thin plates under different temperature distribution (uniform and nonuniform) by using five variable refined plate theory is considered. The most important characteristic of this work is that it contains five unknown displacements of refined plate theory, which is compared with other theories those of the refined four parameters plate theory (RPT), FSDT, HSDT, and Layerwise Theory (LWT) and give good agreement. As a result, the following conclusions may be drawn:

1-The critical temperature obtained for the case of linearly varying temperature (132.76) distribution is about double the critical temperatures for the uniform temperature 57.5329 distribution.

Thermal buckling for uniform temperature rise of simply supported cross-ply (0/90/90/0) laminated plate was compared with FSDT (Shukla, K. K., 2001) it shows discrepancy for (a/h = 4) is 7.8 %. 2- Depending on the lamination scheme used, the critical buckling temperature exhibits a monotonic response with respect to the side to thickness ratio (a/h). This increase/decrease occurs more rapidly with thick (a /h) laminates than with thin laminates as compared with other theories.

3- The critical buckling temperature depends on the lamination scheme, especially for thick laminates, and is greater for [0/90/0], compared to [0/90] laminates, when the same material properties of each layer are used as compared with other theories for present compared [0/90/] with HSDT **(Matsunaga, H., 2005).** It shows a discrepancy of 11.6 %, while for comparison for [0/90/0] with LWT (Cetkvic, M., 2016), it shows 22 %. Especially for thick laminates (a/h = 2).

4- The critical buckling temperature decreases with the increase of the thermal expansion coefficient ratio (α_1/α_2) and is faster for thick, compared to thin laminates.

Again, the increase is greater for thick laminates than for thin laminates. 5- The critical buckling temperature increases with an increase in aspect ratio (a/b). When (a/b > 2), the critical temperature increase is nearly linear and thus identical for all buckling mode shapes.

REFERENCES

- Chen, W. J., Lin, P. D., and Chen, L., W., 1991. Thermal buckling behavior of thick composite laminated plates under nonuniform temperature distribution, *Computers and Structures*, *41*(4), pp. 637-645. DOI: 10.1016/0045-7949(91)90176-M
- Shi, S. H., Hayashi, Y., Petralia, R. S., Zaman, S. H., Wenthold, R. J., Svoboda, K., and Malino W, R., 1999. Thermal post-buckling of composite plates using the finite element modal coordinate method, *Journal of Thermal Stresses*, *22*(6), pp. 595-614, DOI: 10.1080/0149 57399280779
- Mansour, M., Mohieddin, Ghomshei, and Amin, Mahmoudi, 2010. Thermal buckling analysis of cross-ply laminated rectangular plates under nonuniform temperature distribution: A differential quadrature approach, *Journal of Mechanical Science and Technology*, 24(12), pp. 2519-2527, DOI: 10.1007/s12206-010-0918y
- Le-Chung, Shiau, Shih-Yao Kuo, and Cheng-Yuan, Chen, 2010. Thermal buckling behavior of composite laminated plates. Composite Structures, 92(2), pp. 508-514. DOI: 10.1016/j.com pstruct.2009.08.035.
- Jameel, A. N., Sadiq, I. A. and Nsaif, Hasanain, I., 2012. Buckling Analysis of Composite Plates under Thermal and Mechanical Loading, *Journal of Engineering*, 18, November, pp. 1365–90.
- Bourada, M., Tounsi, A., Houari, M. S. A., and Bedia, E. A. A., 2012. A new four-variable refined plate theory for thermal buckling analysis of functionally graded sandwich plates, Journal of Sandwich Structures and Materials, 14(1), pp. 5-33, DOI: 10.1177%2F1099636211426386
- Fazzolari, F. A., Banerjee, J. R., and Boscolo, M., 2013. Buckling of composite plate assemblies using higher order shear deformation theory—An exact method of solution, Thin-Walled Structures, 71, pp 18-34, DOI: open access.city.ac.UK/id/Eprint/14990.
- Fazzolari, F. A., and E., Carrera, 2014. Thermal Stability of FGM Sandwich Plates Under Various Through-the-Thickness Temperature Distributions, Journal of Thermal Stresses, 37(12), pp. 1449-1481, DOI: 10.1080/01495739.2014.937251
- Cetkovic, M., 2016. Thermal buckling of laminated composite plates using layerwise displacement model, *Composite Structures*,142, pp. 238–253. DOI: 10.1016/j.compstruct.2016.01.082
- Xing, Y., and Wang, Z., 2017. Closed form solutions for thermal buckling of functionally graded rectangular thin plates, *Applied Sciences*, 7(12), pp. 1256, DOI: 10.3390/ app7121256
- Vescovini, R. et al., 2017. Thermal buckling response of laminated and sandwich plates using refined 2-D models, *Composite Structures*, 176, pp. 313–328. DOI: 10.1016/j.compstruct.2017.05.021.
- Sadiq, I. A., and Majeed, W., 2019. Thermal buckling of angle-ply laminated plates using new displacement function, *Journal of Engineering*, 25(12), pp. 96–113. DOI: 10.31026/j.eng .2019.12.08.

- Narayan, D., A., M, G., B, P. and M., H., 2019. Investigation of thermo-elastic buckling of variable stiffness laminated composite shells using finite element approach based on higher-order theory. Composite Structures, 211, pp. 24–40. DOI: 10.1016/j.compstruct.2018.12.012
- Emmanuel, Nicholas, P., Dharmaraja, C., Sathya Sofia, A., and Vasudevan, D., 2019. Optimization of laminated composite plates subjected to nonuniform thermal loads, *Polymers and Polymer Composites,27(6)*, pp. 314-322, DOI: 10.1177%2F0967391119846242
- Balakrishna, Adhhikari, and B., N., Singh, 2020. Buckling characteristics of laminated functionally graded CNT-reinforced composite plate under nonuniform uniaxial and biaxial in-plane edge loads, *International Journal of Structural Stability and Dynamics*, 20(2), pp. 2050022, DOI: 10.1142/S0219455420500224
- Kim, S.E., Thai, H.T., and Lee, J., 2009. A two variable refined plate theory for laminated composite plates, *Composite Structures*, 89**(** 2), pp.197–205, DOI.:10.1016/j.compstruct. 2008.07.017
- Reddy, J. N., 2003. Mechanics of Laminated Composite Plates and Shells, *Mechanics of Laminated Composite Plates and Shells*. DOI: 10.1201/b12409.

Appendix

For stiffness cross-ply

$s_{11} = A_{11}\alpha^2 + A_{66}\beta^2$, $s_{12} = (A_{12} + A_{66})\alpha\beta$, $s_{13} = -B_{11}\alpha^3 - (B_{12} + 2B_{66})\alpha\beta^2$, $s_{14} = -B^s_{11}\alpha^3 - (B^s_{12} + 2B^s_{66})\alpha$, $s_{22} = A_{66}\alpha^2 + A_{22}\beta^2$, $s_{23} = -(B_{12} + 2B_{66})\alpha^2\beta - B_{22}\beta^3$, $s_{24} = -(B^s_{12} + 2B^s_{12})\alpha^2\beta - B^s_{22}\beta^3$, $s_{33} = D_{11}\alpha^4 + 2(D_{12} + 2D_{66})\alpha^2\beta^2 + D_{22}\beta^4$, $s_{34} = D^s_{11}\alpha^4 + 2(D^s_{12} + 2D^s_{66})\alpha^2\beta^2 + D^s_{22}\beta^4$, $s_{44} = H^s_{11}\alpha^4 + 2(H^s_{12} + 2H^s_{66})\alpha^2\beta^2 + H^s_{22}\beta^4 + A^s_{55}\alpha^2 + A^s_{44}\beta^2$, $s_{45} = A^a_{55}\alpha^2 + A^a_{44}\beta^2$, $s_{55} = A_{55}\alpha^2 + A_{44}\beta^2$

$A_{16} = A_{26} = D_{16} = D_{26} = D^s_{16} = D^s_{26} = H^s_{16} = H^s_{26} = B_{16} = B_{26} = B^s_{12} = B^s_{16} = B^s_{26} = A_{45} = A^a_{45} = A^s_{45} = 0$

The plane stress reduced stiffness Q_{ij} are Reddy J. N. (2004)

$Q_{11} = \frac{E_1}{1-v_{12}v_{21}}$, $Q_{12} = \frac{v_{12}E_2}{1-v_{12}v_{21}}$, $Q_{11} = \frac{E_2}{1-v_{12}v_{21}}$, $Q_{66} = G_{12}, Q_{44} = G_{23}, Q_{55} = G_{13}$

$\alpha = \frac{m\pi}{a}$, $\beta = \frac{m\pi}{b}$, $and\ (U_{mn}, V_{mn}, W_{bmn}, W_{bmn}, W_{bmn})\ are\ coeficients$

C = $\left(\alpha^2(N^T_x + M^T_x) + \beta^2(N^T_y + M^T_y)\right)$ for linear temperature

C = $(N^T_x\alpha^2 + N^T_y\beta^2)$ for uniform temperature

$$\left(N_x, N_y, N_{xy}\right) = \int_{-\frac{h}{2}}^{\frac{h}{2}} \left(\sigma_x, \sigma_y, \sigma_{xy}\right) dz = \sum_{k=1}^{N} \int_{z_k}^{z_{k+1}} \left(\sigma_x, \sigma_y, \sigma_{xy}\right) dz \,,\, \left(M_x^b, M_y^b, M_{xy}^b\right) = \int_{-\frac{h}{2}}^{\frac{h}{2}} \left(\sigma_x, \sigma_y, \sigma_{xy}\right) z\, dz = \sum_{k=1}^{N} \int_{z_k}^{z_{k+1}} \left(\sigma_x, \sigma_y, \sigma_{xy}\right) z dz \,,\, \left(M_x^s, M_y^s, M_{xy}^s\right) = \int_{-\frac{h}{2}}^{\frac{h}{2}} \left(\sigma_x, \sigma_y, \sigma_{xy}\right) f dz = \sum_{k=1}^{N} \int_{z_k}^{z_{k+1}} \left(\sigma_x, \sigma_y, \sigma_{xy}\right) f\, dz \left(Q_{xz}^a, Q_{yz}^a, Q_{xz}^s, Q_{yz}^s\right) = \int_{-\frac{h}{2}}^{\frac{h}{2}} \left(\sigma_{xz}, \sigma_{yz}, g\sigma_{xz}, g\sigma_{yz}\right) dz = \sum_{k=1}^{N} \int_{z_k}^{z_{k+1}} \left(\sigma_{xz}, \sigma_{yz}, g\sigma_{xz}, g\sigma_{yz}\right) dz$$

$$N^T(\omega) = N_x^T \frac{\partial^2(w_a+w_b+w_s)}{\partial x^2} + N_y^T \frac{\partial^2(w_a+w_b+w_s)}{\partial y^2} + 2N_{xy}^T \frac{\partial^2(w_a+w_b+w_s)}{\partial x \partial y} + M_x^T \frac{\partial^2(w_a+w_b+w_s)}{\partial x^2} + M_y^T \frac{\partial^2(w_a+w_b+w_s)}{\partial y^2} + 2M_{xy}^T \frac{\partial^2(w_a+w_b+w_s)}{\partial x \partial y}$$

$$\alpha_{xx} = \alpha_1 cos^2\theta + \alpha_2 sin^2\theta \,,\, \alpha_{yy} = \alpha_1 sin^2\theta + \alpha_2 cos^2\theta \,,\, 2\alpha_{xy} = 2(\alpha_1 - \alpha_2)\, sin\,\theta\, cos\theta$$

$$\left(A_{ij}, B_{ij}, D_{ij}, B_{ij}^s, D_{ij}^s, H_{ij}^s\right) = \int_{-\frac{h}{2}}^{\frac{h}{2}} \bar{Q}_{ij}(1, z, z^2, f, zf, f^2)\, dz \quad (i,j = 1,2,6), \left(A_{ij}, A_{ij}^a, A_{ij}^s\right) = \int_{-\frac{h}{2}}^{\frac{h}{2}} \bar{Q}_{ij}(1, g, g^2)\, dz \quad (i,j = 4,5)$$